



národní  
úložiště  
šedé  
literatury

**Palaeomagnetic research of cave fill in Hermanshöhle, Austria : final report**

Bosák, Pavel  
2014

Dostupný z <http://www.nusl.cz/ntk/nusl-187418>

Dílo je chráněno podle autorského zákona č. 121/2000 Sb.

Tento dokument byl stažen z Národního úložiště šedé literatury (NUŠL).

Datum stažení: 10.04.2024

Další dokumenty můžete najít prostřednictvím vyhledávacího rozhraní [nusl.cz](http://www.nusl.cz).



# Paleomagnetic research of cave fill in Hermannshöhle, Austria

**Institute of Geology, Academy of Sciences of the Czech Republic, v. v. i.  
Rozvojová 269, 165 00 Praha 6–Lysolaje, Czech Republic**

**Paleomagnetic  
research of cave fill in  
Hermannshöhle,  
Austria.  
Final Report**

**Compiled by:**

**Pavel Bosák**

**Petr Pruner**

**Praha**  
*February 2014*

Institute of Geology, Academy of Sciences of the Czech Republic, v. v. i.  
Rozvojová 269, 165 00 Praha 6–Lysolaje, Czech Republic

# Paleomagnetic research of cave fill in Hermannshöhle, Austria. Final Report




prof. RNDr. Pavel Bosák, DSc.  
Director



ing. Petr Pruner, DSc.\*  
Researcher



Geologický ústav AV ČR, v.v.i.  
Rozvojová 269  
165 00 Praha 6  
(ředitel)



prof. RNDr. Pavel Bosák, DSc.\*\*  
Researcher



\* Certificate on Expert Qualification No. 1920/2004 for planning, pursuing and evaluation of geological activities in geophysics and geological exploration was issued by the Ministry of Environment of the Czech Republic.

\*\* Certificate on Expert Qualification No. 1845/2004 for planning, pursuing and evaluation of geological activities in economic geology and geological exploration was issued by the Ministry of Environment of the Czech Republic.

Institute of Geology of the Academy of Science of the Czech Republic, v. v. i. is registered in register of public research institution on the Ministry of Education, Youths and Sports of the Czech Republic under No. 17113/2006-34/GLÚ.

Trade license to ID No. 67985831 issued by Městská část Praha 6 (Municipality of Prague 6) under No. MCP6 058113/2011.

**Institute of Geology, Academy of Sciences of the Czech Republic, v. v. i.  
Rozvojová 269, 165 00 Praha 6–Lysolaje, Czech Republic**

## **Paleomagnetic research of cave fill in Hermannshöhle, Austria. Final Report**

### **Authors:**

**prof. RNDr. Pavel Bosák, DSc.<sup>1</sup>**

**ing. Petr Pruner, DSc.<sup>1</sup>**

**RNDr. Andrej Mock, PhD<sup>2</sup>**

### **Collaboration:**

#### **Field assistance**

**Mgr. Andrea Schober**

**Lucas Plan, PhD<sup>3</sup>**

### **Palaeomagnetic analysis**

**Mgr. Kristýna Čížková<sup>1</sup>, Jiří Petráček<sup>1</sup>**

<sup>1</sup> Institute of Geology ASCR, v. v. i., Rozvojová 269, 165 00 Praha 6 – Lysolaje, Czech Republic; bosak@gli.cas.cz; pruner@gli.cas.cz

<sup>2</sup> Department of Zoology, Institute of Biological and Ecological Sciences, Faculty of Science, University of Pavel Josef Šafařík, Moyzesova 11, 041 54 Košice, Slovakia

<sup>3</sup> Karst and Cave Department, Museum of Natural History, Messeplatz 1/7a, 1070 Wien, Austria

### **Abstract**

Detailed paleomagnetic analysis of sedimentary profile at Teichkluft showed that sediments are characterized by varying magnetic susceptibilities and NRM with increasing tendency of anisotropy parameter with increase of susceptibility. The component analysis identified 2 short R polarity intervals (0.41 m; 2.19–2.26 m) within samples with the N polarity. Rock magnetic and AMS measurements indicated mostly the presence of oblate, low coercivity magnetic fraction, presumably magnetite. However, the R polarity interval (2.19–2.26 m) revealed also other, higher coercivity fraction (maybe due to hematite/goethite content). The identity of this fraction is still unknown. The R polarity interval in 0.41 m represents a geomagnetic excursion without any doubt. The sedimentary profile with the R polarity interval in 0.41 m must be older than  $162.7 \pm 3.9$  ka old topmost speleothem. The paleomagnetic directions (D, I) are very close to the present magnetic field. Therefore we assume deposition of studied sediments within the Brunhes chron (<780 Ka) and the excursion may be correlated with Jamaica-Pringle Falls (205–215 ka) or Calabrian Ridge 1 excursions (315–325 ka; Langereis et al. 1997). Other Th/U date was obtained at the tourist trail opposite to Teichkluft entrance (ca 495 ka  $\pm$  67/-41 ka) in an altitude corresponding to the top of the Teichkluft profile. This might indicate that the Teichkluft was completely or nearly completely filled twice (before 163 and ca 495 ka) and once completely excavated (between ca 205/325 and ca 495 ka).

The fragments of cuticle of ring-like shape at the level of 2.30 m belongs to attensiid millipedes. The probability that fragments represent *Polyphematia moniliformis* (Latzel, 1884; Diplopoda: Chordeumatida: Attenssiidae) known in the cave is high. It is supposed they are Tertiary relict (Mock and Tajovský 2008). It is not detected, if fragments represent relics of recent/subrecent animal entering open fractures in brown clays close to cave walls, or if they represent really fossil older than ca 163 ka.

### **Zpráva je volně šiřitelná v roce 2015.**

### **Recommended reference:**

Bosák P., Pruner P., Mock A. (2014): *Paleomagnetic research of cave fill in Hermannshöhle, Austria. Final Report.* – Unpublished Report, Inst. Geol. ASCR, v. v. i.: 1–35. Praha.

# 0. CONTENTS

	page
Abstract	4
1. INTRODUCTION	7
2. CAVE POSITION AND SURROUNDINGS	7
3. PROFILE	8
Samples	9
4. PALEOMAGNETIC ANALYSIS	12
Sampling	12
Paleomagnetic analyses and procedures	12
Paleomagnetic and petromagnetic results	13
Discussion	24
5. PALEONTOLOGY	25
6. DISCUSSION OF RESULTS	25
7. CONCLUSIONS	26
<i>Acknowledgement</i>	26
8. REFERENCES	26
Appendix Photo plate	

## List o text tables

*Table 1 Number of samples*

*Table 2 Mean value and standard deviation of the natural remanent magnetisation and volume magnetic susceptibility (MS)*

*Table 3 Principal magnetic parameters of samples, Hermannshöhle*

*Table 4 Mean paleomagnetic directions, Hermannshöhle*

## List of text figures

**Figure 1** Topographic overview map of the cave and its surroundings (from Schober et al. 2013)

**Figure 2** Lower part of sampled profile (samples Nos. HH03 to HH110), Hermannshöhle, Teichkluft (photo by P. Bosák)

**Figure 3** Top of sampled profile with flowstone crust dated to  $162.7 \pm 3.9$  ka (dating sample No. HH5; red cross in photo), Hermannshöhle, Teichkluft (photo by L. Plan)

**Figure 4** Plastic boxes for paleomagnetic samples within the profile, Hermannshöhle, Teichkluft. Numbers means distance in centimeters from profile bottom (photo by P. Bosák)

**Figure 5** Directions of C-components of remanence of samples with normal polarity (left side) and with reverse polarity (right side), Hermannshöhle

**Figure 6** Example of AF demagnetization of sample of sediment (HH033) with normal paleomagnetic polarity, Hermannshöhle

**Figure 7** Example of AF demagnetization of sample of sediment (HH485) with normal paleomagnetic polarity, Hermannshöhle

**Figure 8** Example of AF demagnetization of sample of speleothem (HH230) with normal paleomagnetic polarity, Hermannshöhle

**Figure 9** Example of TD demagnetization of sample of speleothem (HH230) with normal paleomagnetic polarity, Hermannshöhle

**Figure 10** Example of AF demagnetization of sample of sediment (HH041) with reverse paleomagnetic polarity, Hermannshöhle

**Figure 11** Example of AF demagnetization of sample of sediment (HH226) with reverse paleomagnetic polarity, Hermannshöhle

**Figure 12** Anisotropy of magnetic susceptibility, Hermansshöhle

**Figure 13** Basic magnetic and paleomagnetic properties, Hermannshöhle

## Appendix: Photo plate

**Photo 1** Lower segment – samples Nos. HH03 to HH110

**Photo 2** Segment HH03 to HH33

**Photo 3** Segment HH26 to HH58

**Photo 4** Segment HH54 to HH91

**Photo 5** Segment HH74 to HH110

**Photo 6** Lower middle segment – samples Nos. HH115 to HH125

**Photo 7** Lower middle segment – samples Nos. HH219 to HH244  
**Photo 8** Upper middle segment – samples Nos. HH310 to HH389  
**Photo 9** Lower upper segment – samples Nos. HH401 to HH420  
**Photo 10** Topmost segment – samples Nos. HH470 to HH495

## 1. INTRODUCTION

Paleomagnetic research of cave sediments in the Hermannshöhle, Lower Austria, was carried out on September 6, 2013. The sampling was based on agreement of P. Bosák and A. Schober made on June 2013 in Adelsberg (Slovenia).

The sampling profile was carried out in the Teichkluft (behind the lake), at ca 635–640 a. s. l., and was assisted by Pavel Bosák, Petr Pruner, Lucas Plan, Andrea Schober. The aim of the campaign was to obtain additional dating data as Th/U numerical dating yielded dates of ca 100 to more than 600 ka (Schober et al. 2013).

*Table 1 Number of samples*

Cave	Profile	Boxes	Solid	AF	TD
Hermannshöhle	Teichkluft	66	1	67	1

Note: AF = alternating field demagnetization; TD = thermal demagnetization

## 2. CAVE POSITION AND SURROUNDINGS

The chapter is compiled from Schober et al. (2013); for detailed references see the article.

The Hermannshöhle, located near village of Kirchberg am Wechsel (Lower Austria), is one of the biggest caves in the Lower Austroalpine tectonic unit. It developed in an isolated block of weakly metamorphic banded marble. Within only 140 × 160 m ground area and 73 m of elevation difference a total of 4.4 km of corridors formed in a 3-D maze. There are three more caves nearby (Mäanderhöhle, Antonshöhle and Rauchspalten) and it is presumed that all four are genetically related giving a length of almost 5 km (Fig. 1).

The host rocks, foliated, weakly metamorphic calcite marbles, are Middle Triassic carbonates which are part of the Lower Austroalpine Semmering-Wechsel-System, bordered by a Palaeozoic gneiss-and-schist-complex in the north. In the south the area is covered by Neogene and Quaternary sediments of the Kirchberg Basin (580 m a. s. l.), which was formed during the last phase of the Alpine Orogeny due to lateral extrusion. The basin is linked to branches of one of the largest strike-slip fault in Austria, the Salzachtal-Ennstal-Mariazell-Puchberg-Fault and the Mur-Mürz-Fault, respectively.

The cave ranges from about 600 m to 680 m a. s. l. Although the overall volume of passages is roughly only 17,000 m<sup>3</sup> (1 % of the neighboring host rock) the cumulative length and density of corridors are remarkable. The corridors developed along prominent fault directions and NW–SE-striking corridors are the most abundant. Most are sub-horizontal with almost no inclination and some are inclined between 40 and 60° but only very few are subvertical. The second main strike direction is NE-SW, which is nearly perpendicular to the first one with more or less horizontal corridors.

So far nine speleothem samples were dated by the U/Th method. Except for one recent flowstone (ca. 1 ka), all samples are rather old, ranging from 100 to ca 500 ka. Two of the samples are out of range and are probably older than 600 ka. Surprisingly, these old ages were found in the middle cave level which is 45 and 60 m, respectively, above the Kirchberg Basin, which forms the base level of the karst system and only 25 and 40 m above Rams Brook, which potentially fed the system in former times.



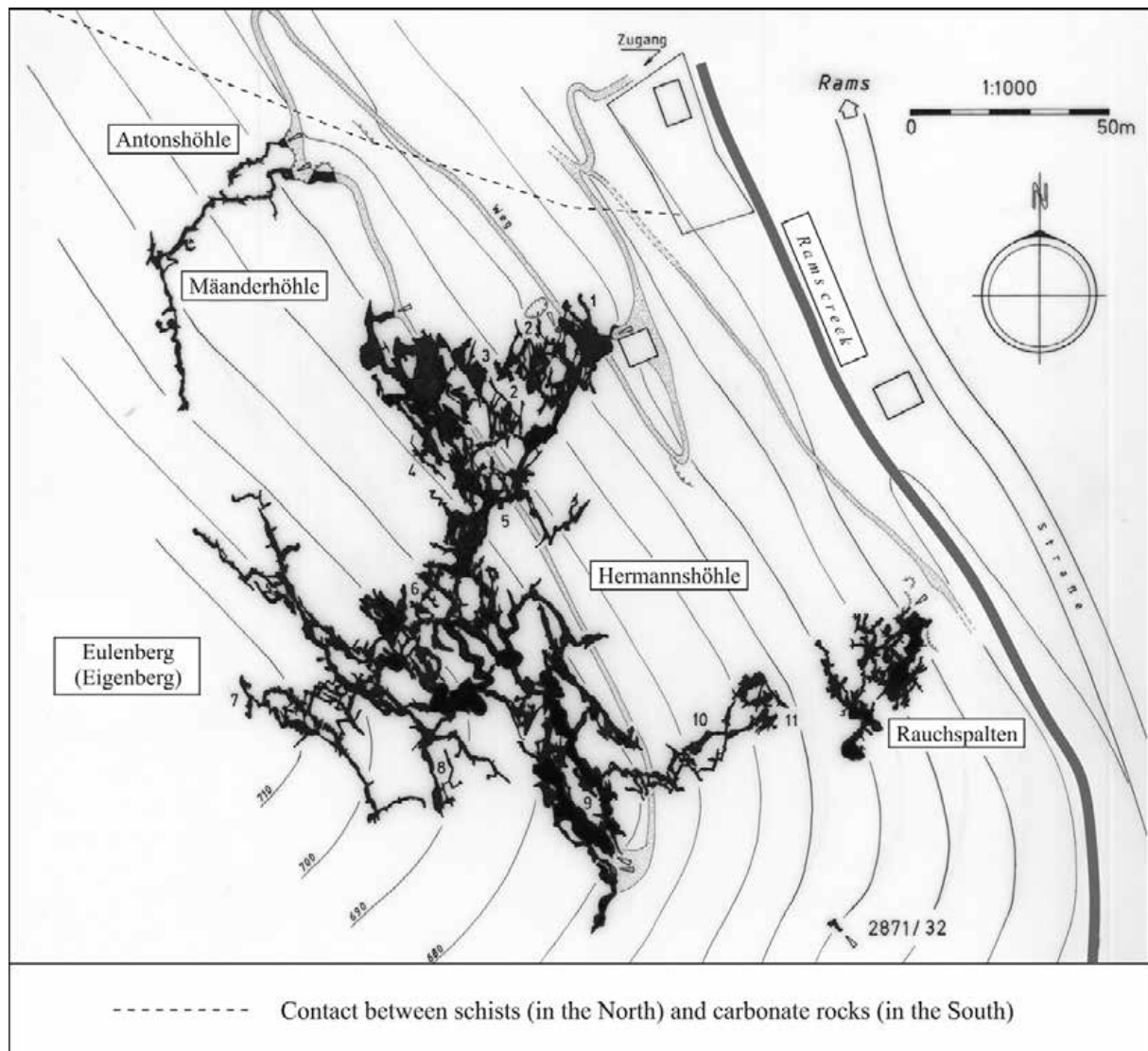


**Figure 1** Topographic overview map of the cave and its surroundings (from Schober et al. 2013)

### 3. PROFILE

The sampled profile consisted from several parts – segments where sampling for paleomagnetic analysis was possible (see also Appendix).

Complicated sequence of multi(vario)-colored clays (brown and violet colors prevail) with yellow micaceous clayey sands (Fig. 2). Abundant Mn-rich schlieren pinch out from cave walls into the sediment. Cave walls are usually highly corroded, in places up to sandy residuum. Small erosion surfaces are often stained/coated by Fe-Mn compounds. Erosion channels filled with cubes of brown clays with yellowish-sandy matrix occur in the upper part of the profile. Whole profile is highly disturbed by old excavations and digging.

The profile is covered by flowstone crust dated to  $162.7 \pm 3.9$  ka (dating sample No. HH5; Fig. 3).



**Figure 2** Lower part of sampled profile (samples Nos. HH03 to HH110), Hermannshöhle, Teichkluft (photo by P. Bosák)

## Samples

Numbers: from below up; zero at the profile base. Totally 66 boxes and 1 solid sample (speleothem; see Appendix No. 1, Figures 1 to 10) were taken.

### Samples marked: HH

Upper segment +175 cm above dated stalagmite (ca 163 ka), narrow between cave walls

HH 495	307/85
HH 489	307/85
HH 485	307/85
HH 480	307/87
HH 474	334/85
HH 470	334/85
HH 420	50/88
HH 414	dtto
HH 406	dtto
HH 401	50/88

Excavation at right cave wall about +90 above HH 230

Bedding approximately horizontal

HH 389	339/89
HH 386	339/89
HH 381	320/85
HH 377	337/86
HH 370	dtto
HH 367	337/86
HH 362	337/81

HH 357	337/86
HH 354	327/82
HH 350	331/87
HH 341	340/84
HH 337	331/86
HH 330	331/81
HH 325	331/90
HH 318	327/88
HH 314	dtto
HH 310	327/88

Profile parallel with cave wall, at the left with speleothem

Bedding in clays 231/35

HH 244	238/85	
HH 240	238/85	
HH 237	228/83	
HH 230	168/40	speleothem, solid sample, bedding
HH 226	224/89	
HH 224	224/89	
HH 220	224/90	not on photo, additional sample,
HH 219	235/89	contains weathered underlying limestone
HH 125	330/87	
HH 121		
HH 119		
HH 115	330/87	

Lower profile

bedding	70/18
HH 110	335/87
HH 107	
HH 103	
HH 99	
HH 95	
HH 91	
HH 88	335/87
HH 84	324/86
HH 79	320/87
HH 74	326/85
HH 71	
HH 67	
HH 63	326/85
HH 58	325/90
HH 54	
HH 50	
HH 46	325/90
HH 41	313/85
HH 37	320/88
HH 33	327/88
HH 30	329/84
HH 26	320/86
HH 23	328/88
HH 19	
HH 15	
HH 12	328/88
HH 08	320/89
HH 02	320/89





**Figure 3** Top of sampled profile with flowstone crust dated to  $162.7 \pm 3.9$  ka (dating sample No. HH5; red cross in photo), Hermannshöhle, Teichkluff (photo by L. Plan)



## 4. PALEOMAGNETIC ANALYSIS

For detailed description of methodology of sampling and data acquisition, processing and interpretation see Zupan Hajna et al. (2008, pp. 38–44).

### Sampling

The high-resolution sampling of profiles (Bosák, Pruner and Kadlec 2003; Zupan et al. 2008) was adopted in the Hermannshöhle Cave; centers of samples are 2 to max. 7 cm distant.

Unconsolidated samples were sampled by use of boxes (Fig. 4) made from non-magnetic plastics (Natsuhara Giken Co., Ltd., Japan) with external size of 20 x 20 x 20 mm and internal volume of about 6.7 cm<sup>3</sup>. Samples from speleothems were collected in large oriented pieces. All field hand specimens were oriented *in situ*: the direction of dip was measured by the geological compass and the direction of north was drawn on the sample.



**Figure 4** Plastic boxes for paleomagnetic samples within the profile, Hermannshöhle, Teichkluft. Numbers means distance in centimeters from profile bottom (photo by P. Bosák)

### Paleomagnetic analyses and procedures

Paleomagnetic analyses were completed in the Laboratory of Paleomagnetism, IG ASCR, v. v. i. in Praha–Průhonice. Totally 69 samples were demagnetized by alternating field (AF) and 2 solid samples (from speleothem) demagnetized thermally (TD). Procedures were selected to allow the separation of the respective components of the remanent magnetization (RM) and the determination of their geological origin. Oriented hand sample was cut into cubes of 20 x 20 x 20 mm and subjected to the AF and/or TD. Samples from unconsolidated

sediments were demagnetized only by the AF. The natural remanent magnetization (NRM) was measured on 2G Superconducting Rock Magnetometer with incorporated AF unit and tested by the progressive TD using the MAVACS apparatus. The MAVACS secures the generation of a high-magnetic vacuum in a medium of thermally-demagnetized specimens (Příhoda et al. 1989). The all specimens were subjected to AF demagnetization up to a field of 100 mT in 12–16 steps and/or TD method in 11–15 fields. Volume magnetic susceptibility (MS) was measured on a KLY-4 kappa-bridge (Jelínek 1973). The NRM is identified by the symbol  $J_n$ , the corresponding remanent magnetic moment by the symbol  $M$ . Graphs of normalized values of  $M/M_0 = F(t)$  were constructed for each analyzed specimen. To test the possible influence of phase changes of magnetic minerals during laboratory TD processing, diagrams of  $k_t/k_n$  values vs laboratory thermal demagnetizing field  $t$  (°C) were also constructed for samples. The volume magnetic susceptibility of the sample subjected to TD at temperature  $t$  (°C) and cooled to room temperature is denoted by symbol  $k$ .

An isothermal remanent magnetization (IRM) was acquired progressively using a Magnetic Measurements MPM10 pulse magnetizer in fields up to 1 T. The acquired IRM was measured after each imparted field with an Agico JR-5 spinner magnetometer. Seven pilot samples were subjected to the analysis of IRM acquisition and AF demagnetization curves with the aim to establish magnetic hardness of the magnetically active minerals contained in the sediments.

As a complementary technique to magnetostratigraphy, the measurements of the anisotropy of the low-field magnetic susceptibility (AMS) were performed throughout the section. The AMS was measured with an Agico KLY-4S Kappabridge with an alternating field intensity of 300 A.m<sup>-1</sup> and operating frequency of 875 Hz. The AMS of any rock is dependent on the intrinsic magnetic susceptibility, volume fraction, and degree of preferred orientation of the individual rock-constituent minerals (Jelínek 1981).

Multi-component analysis technique of Kirschvink (1980) was applied to separate the respective NRM components. Fisher statistics (1953) were employed for the calculation of mean directions of the characteristic components of remanent magnetization (ChRM) derived by the multi-component analysis.

## Paleomagnetic and petromagnetic results

Totally 68 oriented laboratory samples were studied for their palaeomagnetic properties (Tab. 3). Studied sediments are characterized by the NRM intensity from 0.31 to 44.79 mA.m<sup>-1</sup> and the MS values from 58.65 to 1392.93 x 10<sup>-6</sup> SI units. The mean values of NRM and MS moduli are documented in Table 2.

*Table 2 Mean value and standard deviation of the natural remanent magnetisation and volume magnetic susceptibility (MS)*

Hermannshöhle	NRM [mA.m <sup>-1</sup> ]	MS x10 <sup>-6</sup> [SI]	Interval [m]*
Mean value	13.501	526.7	0.02 – 4.95
Standard deviation	11.073	360.5	
Number of samples	68	68	

\* from base to top

The multi-component analysis of the remanence shows that the samples have a two-component RM. The A-component is undoubtedly of viscous (weathering) origin and can be demagnetized in the AF (0–5 up to 10 mT). The C-component is the most stable, with demagnetization in the AF (15–40 up to 100 mT). Five samples could not be determined by C-component. The stereographic projections of the C-component (ChRM) with N and R polarity are shown on Figure 5.

*Table 3 Principal magnetic parameters of samples, Hermannshöhle*

Sample number	Position [cm]	NRM [A.m <sup>-1</sup> ]	MS [10 <sup>-6</sup> SI]	D [deg]	I [deg]	Polarity
HH002	2	12.52	464.40	85.5	78.1	N
HH008	8	25.08	1096.83	95.6	64.3	N
HH012	12	1.25	205.87	-	-	-
HH015	15	15.95	668.14	76.4	64.2	N
HH019	19	19.31	763.27	79.9	68.3	N
HH023	23	14.87	683.09	357.1	49.4	N
HH026	26	19.01	703.80	337.7	63.4	N
HH030	30	3.20	214.94	38.9	59.5	N
HH033	33	2.47	172.30	339.9	39.1	N
HH037	37	3.25	204.92	19.2	64.9	N
HH041	41	1.02	188.32	162.7	-37.6	R
HH046	46	15.92	642.2	7.2	47.1	N
HH050	50	10.55	554.97	329.8	49.9	N
HH054	54	11.47	563.51	21.2	54.8	N?
HH058	58	19.59	900.13	19	60.1	N
HH063	63	25.27	954.52	43.3	51.1	N
HH067	67	21.75	767.19	14.7	55.4	N
HH071	71	26.64	887.19	12.1	42.5	N
HH074	74	44.79	1313.98	17.8	49.3	N
HH079	79	24.58	948.67	1.9	44.9	N
HH084	84	20.58	936.71	358.6	65.9	N
HH088	88	9.01	448.54	15.8	53.5	N
HH091	91	3.99	228.66	26.3	52.1	N
HH095	95	7.37	313.82	353.6	51.5	N
HH099	99	19.08	537.43	346.1	64.4	N
HH103	103	3.37	132.28	349.2	58.2	N
HH107	107	0.83	113.29	-	-	-
HH110	110	2.02	120.14	354.2	32.6	N
HH115	115	0.49	82.40	-	-	-
HH119	119	1.23	93.35	358.3	34.8	N
HH121	121	0.98	92.78	202.0	78.4	N?
HH125	125	2.03	87.13	311.2	22.4	N?
HH219	219	2.49	249.56	172.1	-24.7	R
HH220	220	1.17	192.45	173.0	-29.4	R
HH224	224	2.05	149.61	181.2	-17.0	R
HH226	226	0.31	103.91	167.1	-27.1	R
HH237	237	2.05	58.65	337.8	60.1	N
HH240	240	5.90	127.55	352.7	57.7	N
HH244	244	5.10	122.96	347.9	53.0	N
HH310	310	28.00	904.84	359.5	65.8	N
HH314	314	29.64	1139.76	5.8	53.3	N
HH318	318	16.19	700.82	4.7	37.1	N

Sample number	Position [cm]	NRM [A.m <sup>-1</sup> ]	MS [10 <sup>-6</sup> SI]	D [deg]	I [deg]	Polarity
HH330	330	33.09	1148.52	1.5	41.7	N
HH337	337	44.29	1392.93	20.8	45.4	N
HH341	341	6.96	321.31	4.8	43.1	N?
HH350	350	6.49	324.67	-	-	-
HH354	354	14.04	507.20	344.2	56.8	N?
HH357	357	23.21	721.47	355.2	26.9	N?
HH362	362	3.42	208.40	315.5	31.4	N?
HH367	367	5.88	278.44	355.9	39.1	N?
HH370	370	5.57	310.87	326.3	47.5	N
HH377	377	36.79	1089.06	0.8	31	N
HH381	381	19.16	674.68	337.3	31.5	N
HH386	386	17.90	587.98	349.6	47.8	N
HH389	389	3.36	143.67	354.6	49.4	N
HH401	401	9.35	353.60	7.7	54.7	N
HH406	406	11.74	409.87	31.3	58.8	N?
HH414	414	5.84	358.46	46.8	55.5	N?
HH420	420	9.90	529.49	-	-	-
HH470	470	21.05	957.83	349.9	39.6	N?
HH474	474	31.63	1314.37	316	65.4	N?
HH480	480	24.07	848.57	2.9	46.3	N
HH485	485	17.26	574.65	353.7	52.7	N
HH489	489	15.71	440.83	0.9	50.5	N
HH495	495	20.56	536.67	347.3	58.4	N

Explanation: N – normal; R – reverse; N? – normal, unclear

Table 4 summarizes results of the mean direction of samples from this profile. The mean paleomagnetic directions of C-components for the normal polarity are  $D = 2^\circ$ ,  $I = 56^\circ$  and for reverse polarity part are  $D = 171^\circ$ ,  $I = -28^\circ$ . The examples of AF demagnetization of samples (sediments – position HH33 and HH485 cm) and (speleothem – position HH230 cm) with normal (N) paleomagnetic polarity are presented in Figures 6, 7 and 8. Result of TD demagnetization is documented of sample (speleothem – position HH230 cm) on Figure 9. Figures 10 and 11 represent examples of samples (sediments – position HH41 and HH226 cm) with reverse (R) polarity.

*Table 4 Mean paleomagnetic directions, Hermannshöhle*

Sample No.	Polarity	Mean paleomagnetic directions		$\alpha_{95} [^\circ]$	$k$	$n$
		$D [^\circ]$	$I [^\circ]$			
HH002–495	N	1.98	55.69	4.96	13.04	61
HH041; 220–226	R	171.45	-27.95	9.49	54.24	4

Note: N – normal polarity, R – reverse polarity; D, I – declination and inclination of the remanent magnetisation after dip correction;  $\alpha_{95}$  – semi-vertical angle of the cone of confidence calculated according to Fischer (1953) at the 95% probability level; k – precision parameter; n – number of analyzed samples



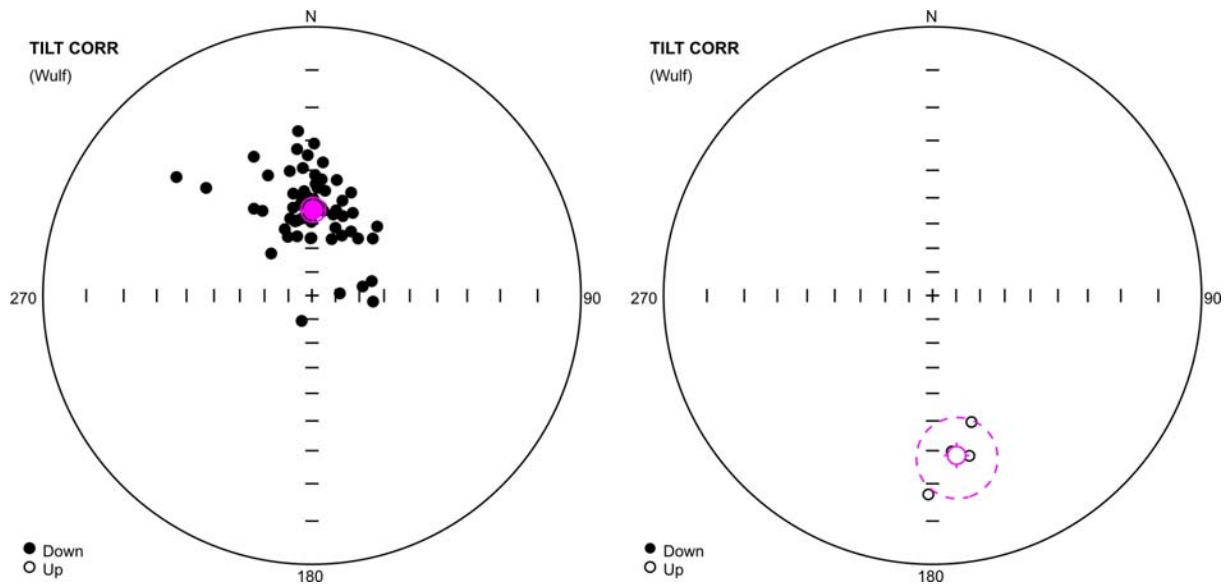


**Figure 5** Directions of C-components of remanence of samples with normal polarity (left side) and with reverse polarity (right side), Hermannshöhle

Stereographic projection, open (full) small circles represent projection onto the lower (upper) hemisphere. The mean direction calculated according to Fisher (1953) is marked by a crossed circle, the confidence circle at the 95% probability level is circumscribed about the mean direction.

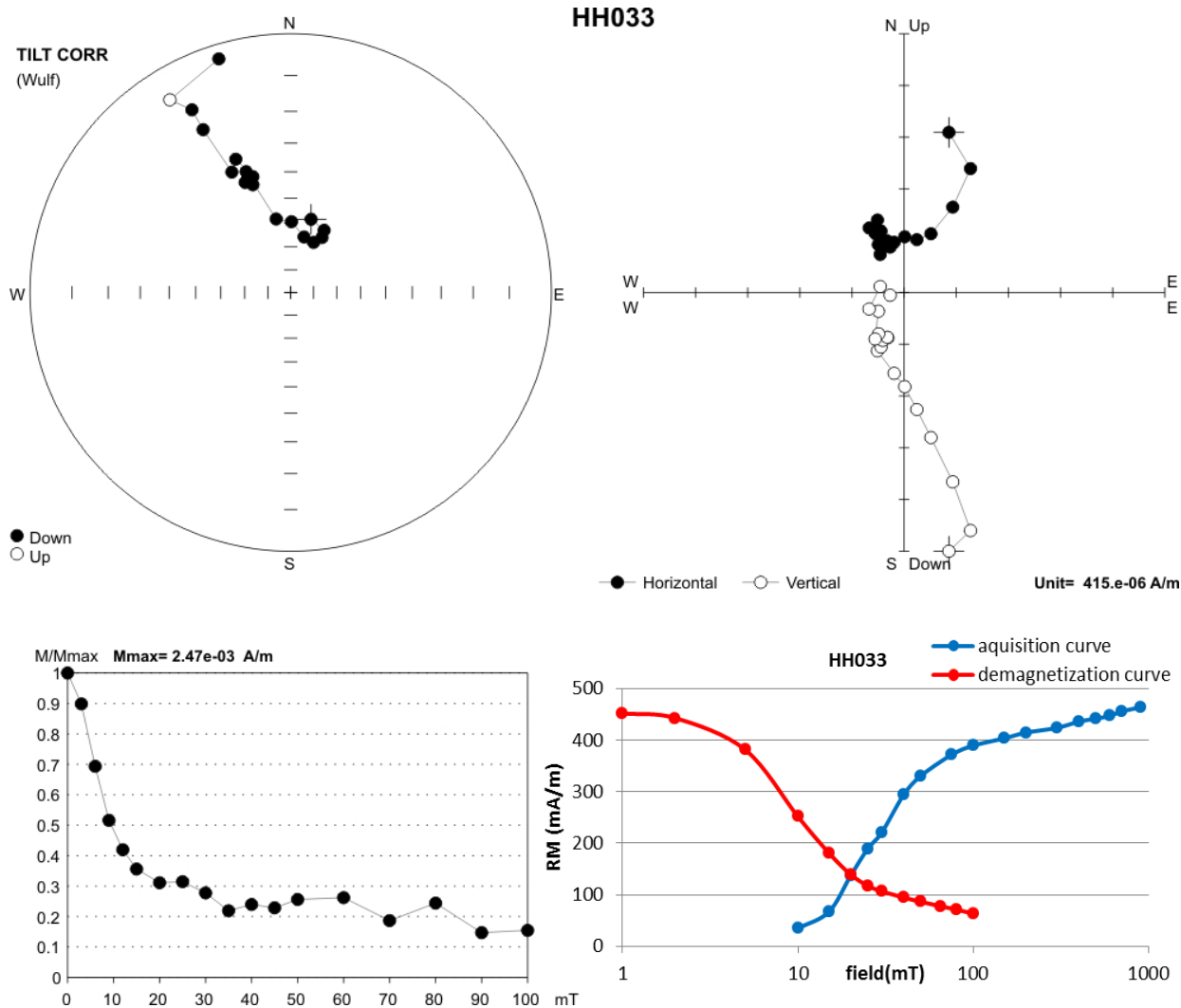


**Figure 6** Example of AF demagnetization of sample of sediment (HH033) with normal paleomagnetic polarity, Hermannshöhle

Note: Top left – A stereographic projection of the natural remanent magnetization of a sample in the natural state (cross section) and after progressive AF demagnetization. Top right – Zijderveld diagram – solid circles represent projection on the horizontal plane (XY), open circles represent projections on the north–south vertical plane (XZ). Bottom left – A graph of normalized values of the remanent magnetic moments versus demagnetizing fields;  $M$  – modulus of the remanent magnetic moment of a sample subjected to AF demagnetization. Bottom right – IRM acquisition and following AF demagnetization curves.

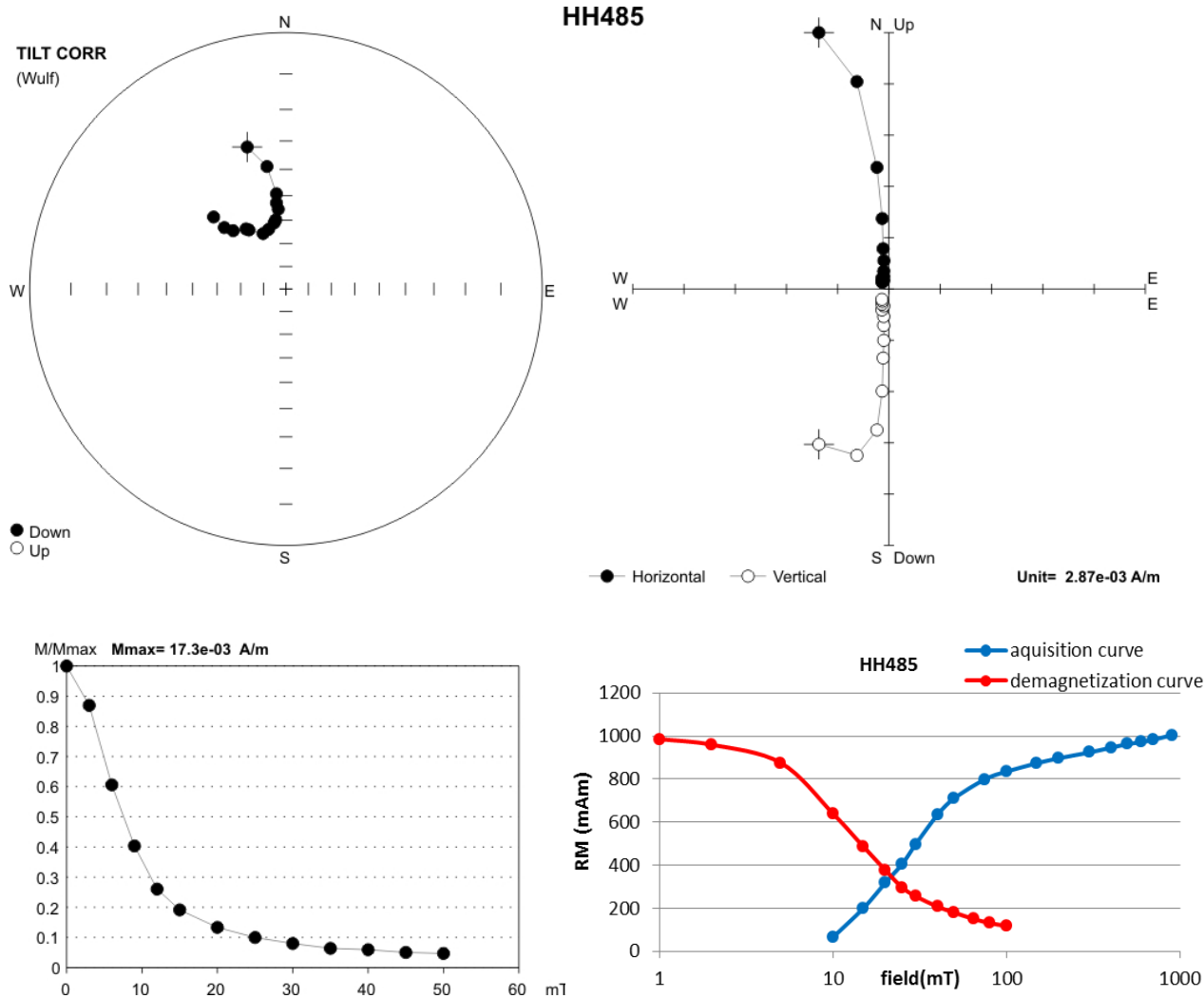


**Figure 7** Example of AF demagnetization of sample of sediment (HH485) with normal paleomagnetic polarity, Hermannshöhle

Note: Top left – A stereographic projection of the natural remanent magnetization of a sample in the natural state (cross section) and after progressive AF demagnetization. Top right – Zijderveld diagram – solid circles represent projection on the horizontal plane (XY), open circles represent projections on the north–south vertical plane (XZ). Bottom left – A graph of normalized values of the remanent magnetic moments versus demagnetizing fields;  $M$  – modulus of the remanent magnetic moment of a sample subjected to AF demagnetization. Bottom right – IRM acquisition and following AF demagnetization curves.

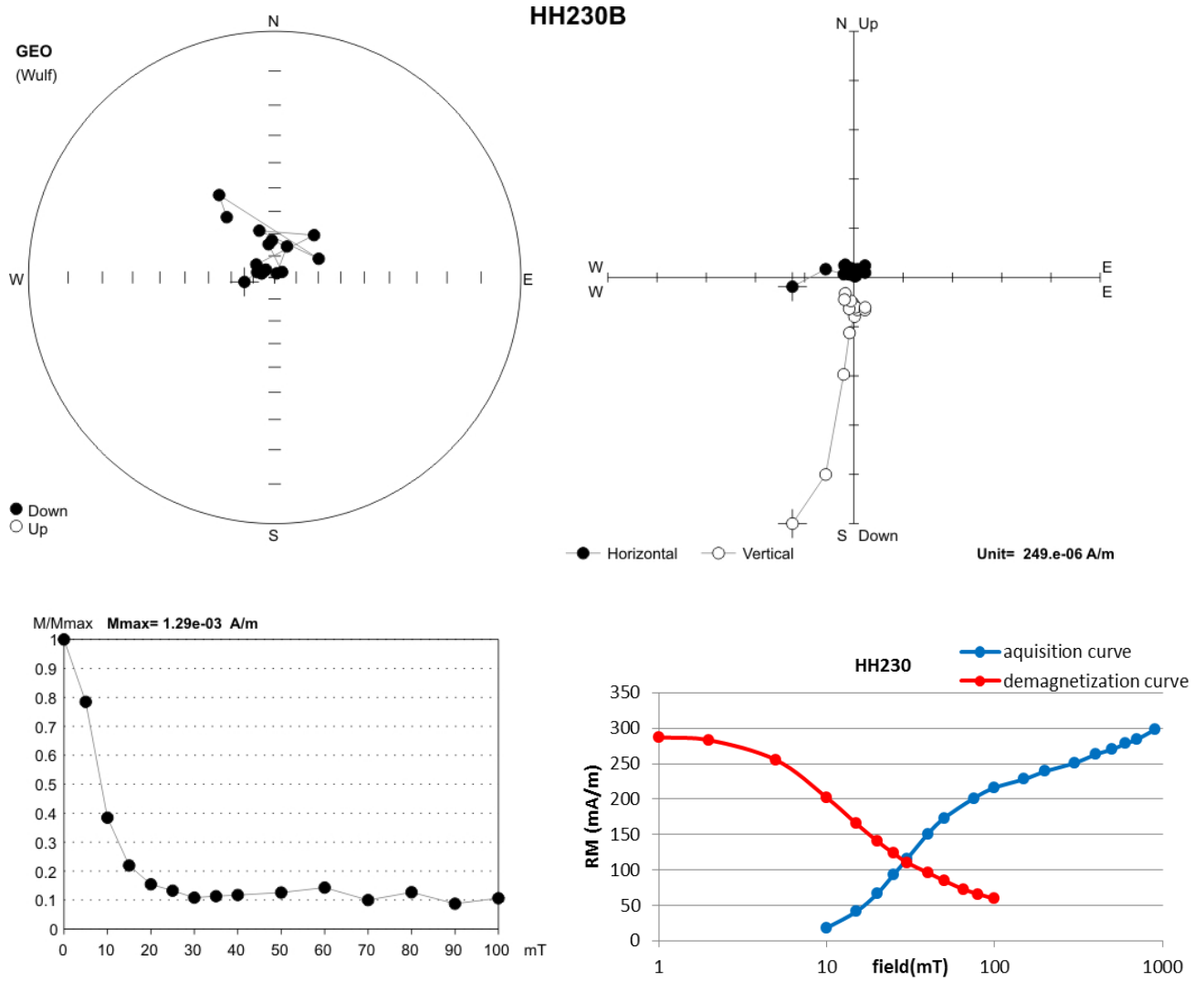


**Figure 8** Example of AF demagnetization of sample of speleothem (HH230) with normal paleomagnetic polarity, Hermannshöhle

Note: Top left – A stereographic projection of the natural remanent magnetization of a sample in the natural state (cross section) and after progressive AF demagnetization. Top right – Zijderveld diagram – solid circles represent projection on the horizontal plane (XY), open circles represent projections on the north–south vertical plane (XZ). Bottom left – A graph of normalized values of the remanent magnetic moments versus demagnetizing fields;  $M$  – modulus of the remanent magnetic moment of a sample subjected to AF demagnetization. Bottom right – IRM acquisition and following AF demagnetization curves.

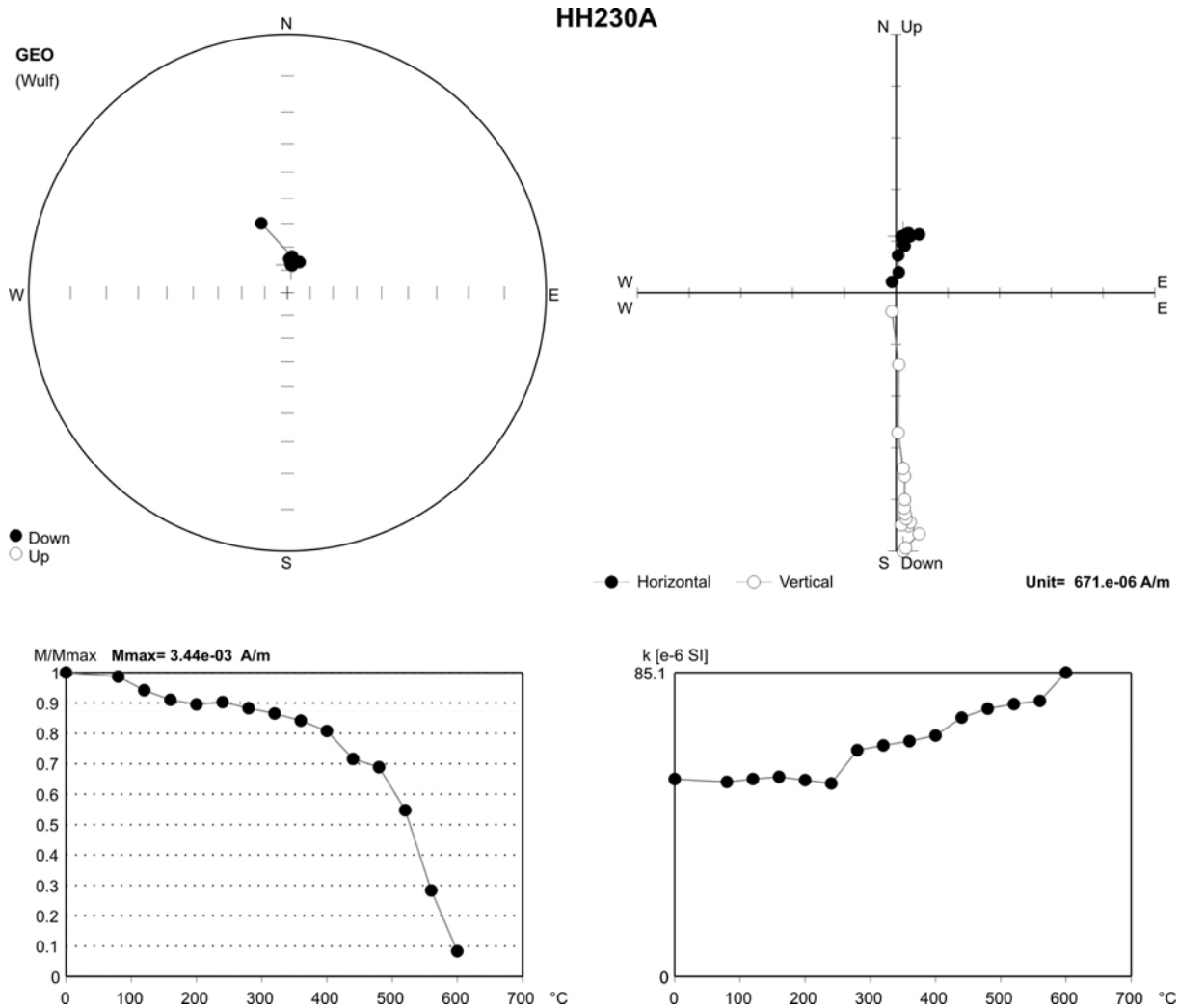


**Figure 9** Example of TD demagnetization of sample of speleothem (HH230) with normal paleomagnetic polarity, Hermannshöhle

Note: Top left – A stereographic projection of the natural remanent magnetization of a sample in the natural state (cross section) and after progressive TD demagnetization. Top right – Zijderveld diagram – solid circles represent projection on the horizontal plane (XY), open circles represent projections on the north–south vertical plane (XZ). Bottom left – A graph of normalized values of the remanent magnetic moments versus temperature;  $M$  – modulus of the remanent magnetic moment of a sample subjected to TD demagnetization. Bottom right – the bulk magnetic susceptibility depending on the temperature achieved during the previous heating step.

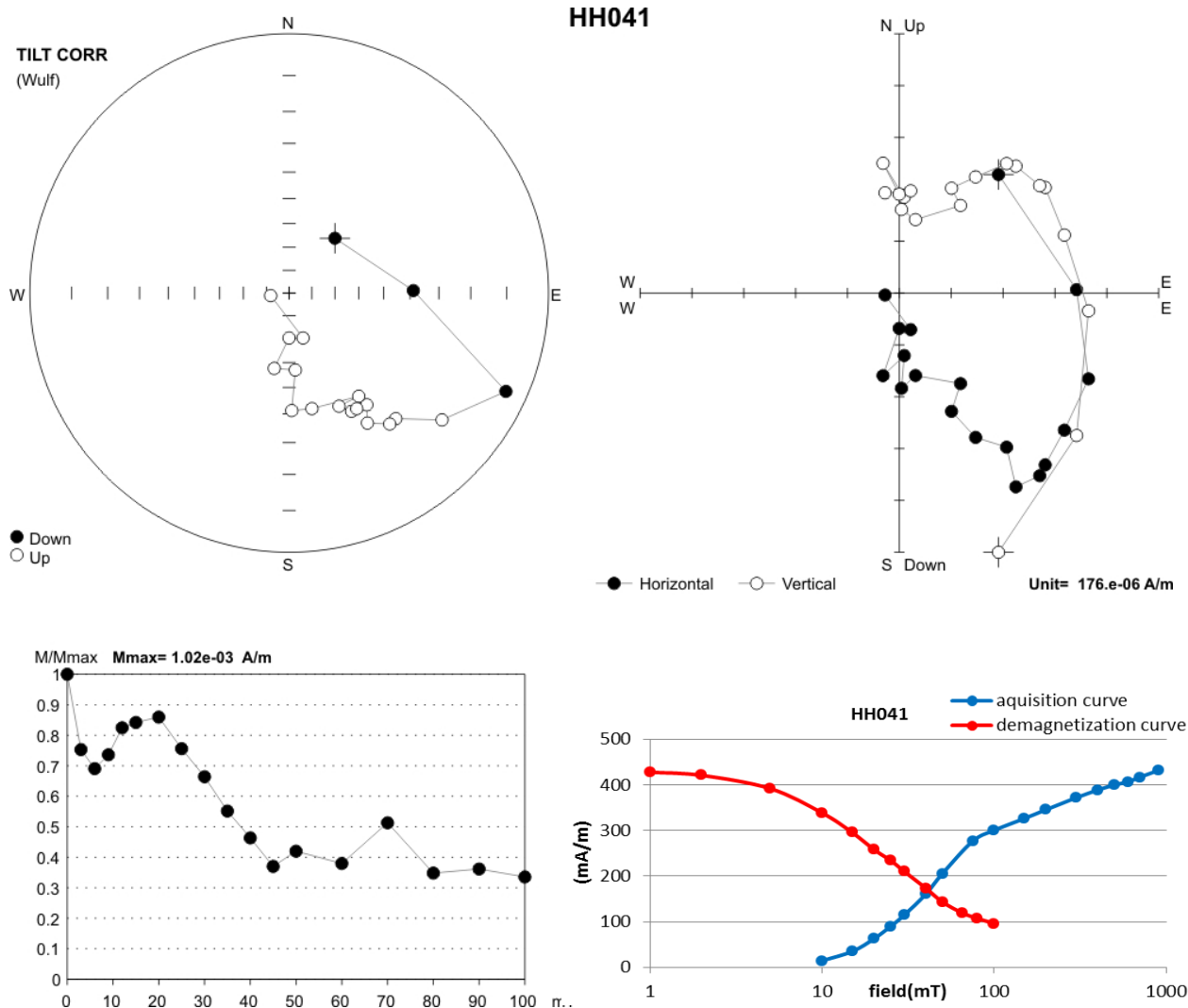


**Figure 10** Example of AF demagnetization of sample of sediment (HH041) with reverse paleomagnetic polarity, Hermannshöhle

Note: Top left – A stereographic projection of the natural remanent magnetization of a sample in the natural state (cross section) and after progressive TD demagnetization. Top right – Zijderveld diagram – solid circles represent projection on the horizontal plane (XY), open circles represent projections on the north–south vertical plane (XZ). Bottom left – A graph of normalized values of the remanent magnetic moments versus temperature;  $M$  – modulus of the remanent magnetic moment of a sample subjected to TD demagnetization. Bottom right – the bulk magnetic susceptibility depending on the temperature achieved during the previous heating step.

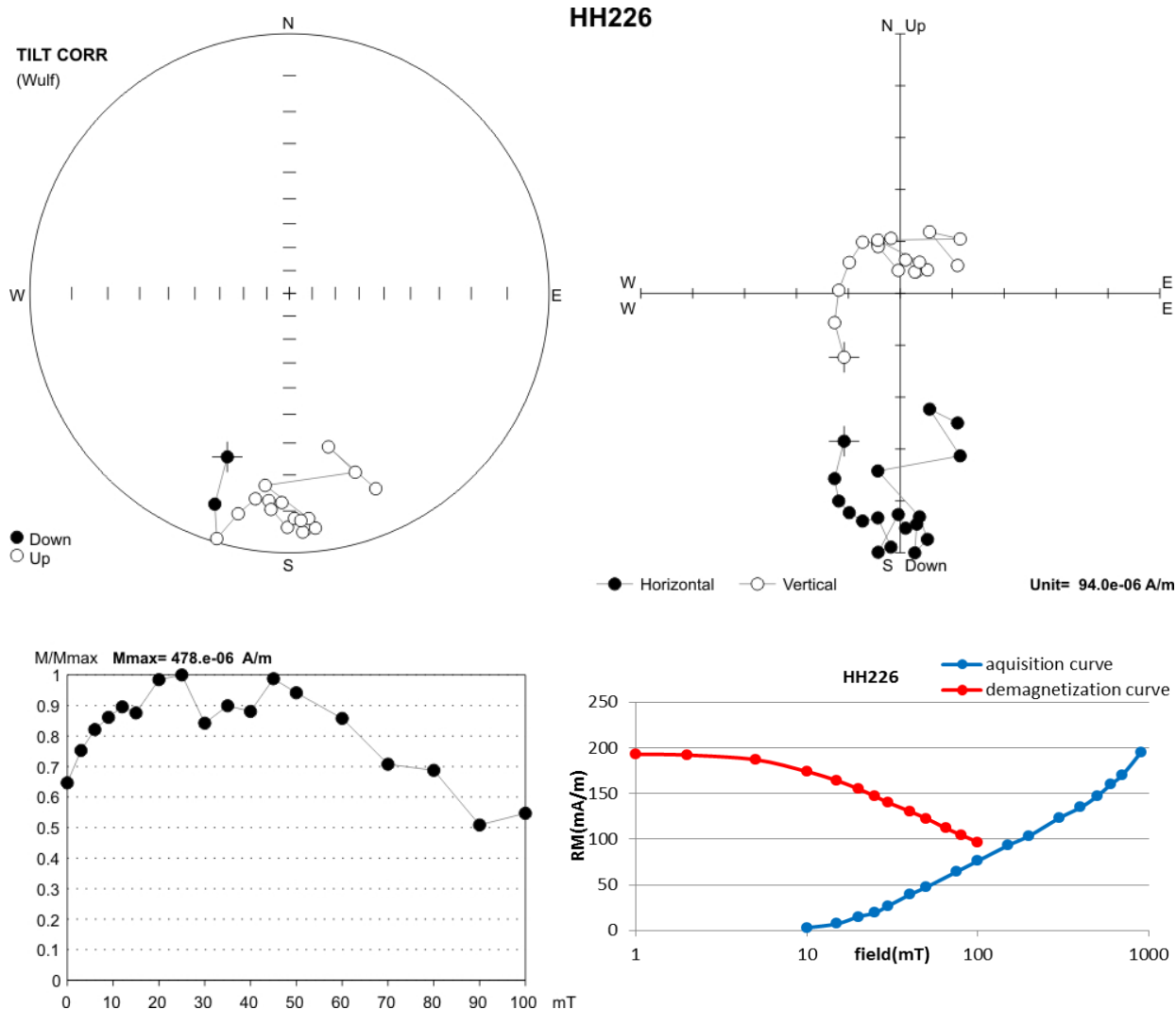


**Figure 11** Example of AF demagnetization of sample of sediment (HH226) with reverse paleomagnetic polarity, Hermannshöhle

Note: Top left – A stereographic projection of the natural remanent magnetization of a sample in the natural state (cross section) and after progressive AF demagnetization. Top right – Zijderveld diagram – solid circles represent projection on the horizontal plane (XY), open circles represent projections on the north–south vertical plane (XZ). Bottom left – A graph of normalized values of the remanent magnetic moments versus demagnetizing fields;  $M$  – modulus of the remanent magnetic moment of a sample subjected to AF demagnetization. Bottom right – IRM acquisition and following AF demagnetization curves.

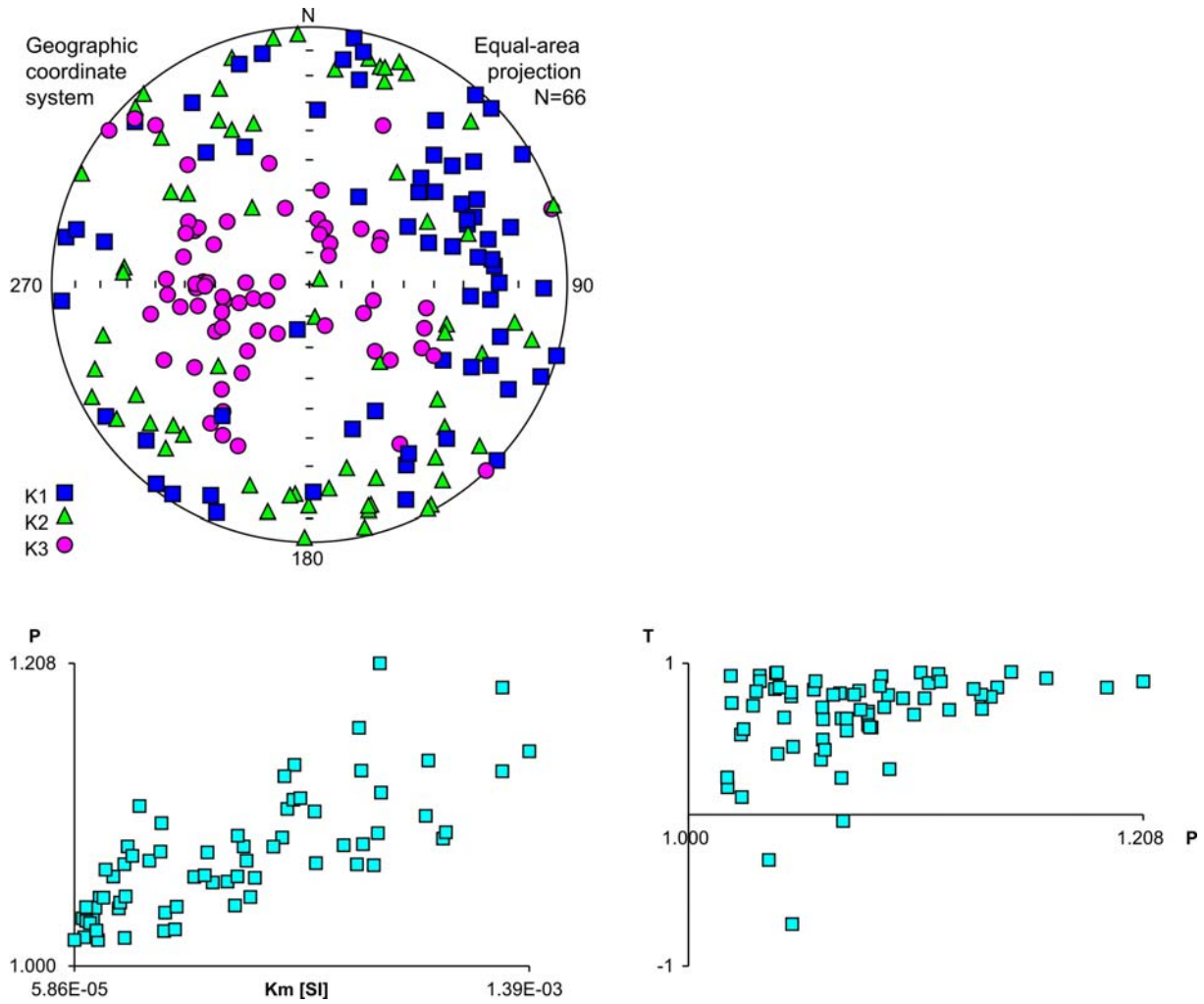


**Figure 12** Anisotropy of magnetic susceptibility, Hermannshöhle

Note: Top left diagram – the projection of the longest  $k_1$  axis (squares)  $k_2$  middle axis (triangles) and the shortest  $k_3$  (circles) axis of the AMS ellipsoid to the lower projection hemisphere. Bottom left diagram – AMS degree (P) versus bulk MS (Km). Bottom right diagram – AMS shape (T) versus AMS degree (P).

Results of anisotropy of magnetic susceptibility (AMS) are presented on Figure 12. The systematic acquisition of paleomagnetic data within a studied section allowed the construction of a detailed magnetostratigraphic profile with a high resolution (Fig. 13). In intervals with polarity change, the frequency of sampling was so high that an almost continuous record of the magnetic and paleomagnetic parameters was obtained. Each magnetostratigraphic profile contains several columns with values of volume MS, the NRM moduli values (M) of samples in the natural state, paleomagnetic directions D and I (of the ChRM-components of the RM inferred by multi-component analysis), discriminant function of polarity zones (Man 2008) and polarity scale.



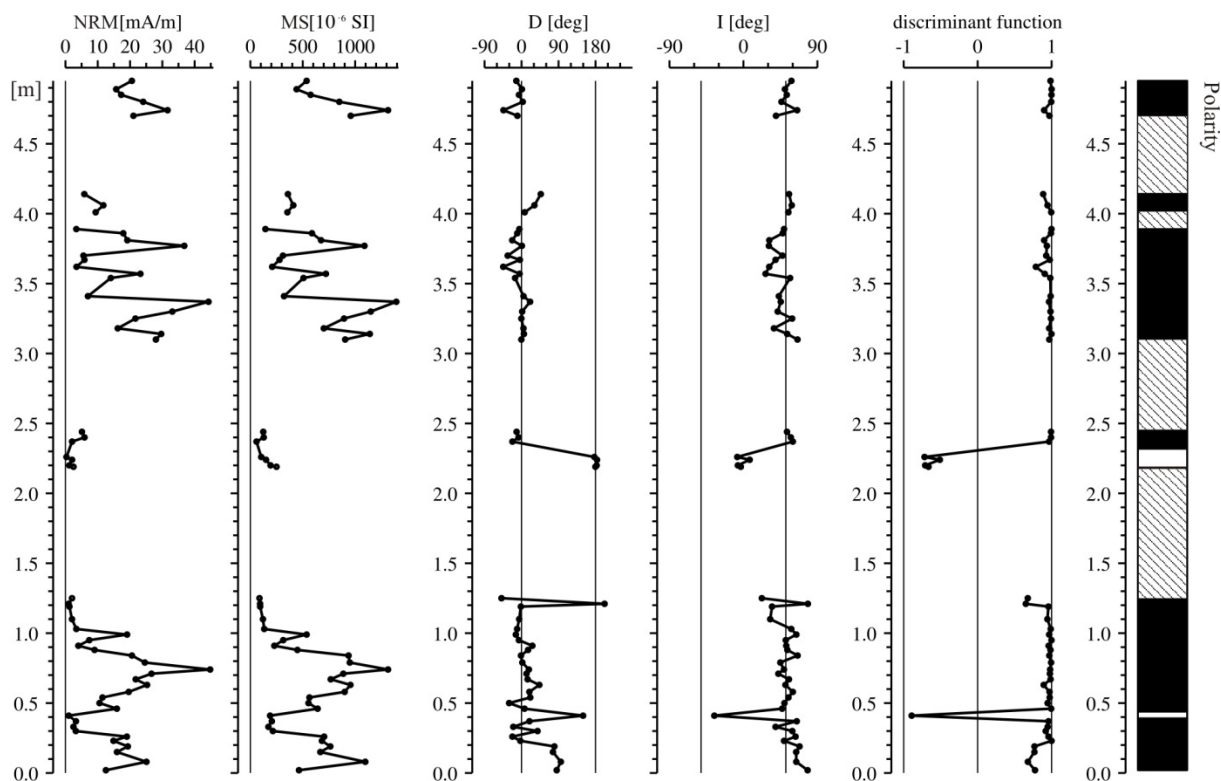


**Figure 13** Basic magnetic and paleomagnetic properties, Hermannshöhle

Note: natural remanent magnetization – NRM; volume magnetic susceptibility – MS; paleomagnetic declination – D; paleomagnetic inclination – I; discriminant function of polarity zones; white – R polarity; black – N polarity; hatched – no samples

## Discussion

The AF and also TD allowed separation of remanent magnetization components and to determine their geologic origin. Results of the measurements show that the sediments are characterized by varying magnetic susceptibilities and NRM with increasing tendency of anisotropy parameter with increase of susceptibility. The component analysis revealed 2 short R polarity intervals (0.41 m; 2.19–2.26 m) within samples with the N polarity. In sedimentary rocks unaffected by tectonic ductile deformation, the so-called „normal magnetic fabric“ is usually observed. The normal magnetic fabric is characterized by magnetic foliation oriented parallel to the bedding, and magnetic lineation being roughly parallel to the near-bottom water current direction or, in special cases, perpendicular to it. Rock magnetic and AMS measurements indicated mostly the presence of oblate, low coercivity magnetic fraction, presumably magnetite. However, the R polarity intervals (2.19–2.26 m) revealed also another, higher coercivity fraction. The identity of this fraction is still unknown and needs further magnetomineralogical studies (i. e. temperature-dependent magnetic susceptibility, coercivity spectra, etc.).

Components of the geomagnetic field calculated for the geographic coordinates of cave for the January of year 2014 are: magnetic declination was 3.53° E and magnetic inclination 62.63° N. Table 4 documents mean paleomagnetic data including mean paleomagnetic D and I for the section of the N polarity. Studied profiles showed N polarized magnetization and two very short R polarity intervals (excursions). The R polarity interval in 0.41 m represents a geomagnetic excursion without any doubt. It must be older than  $162.7 \pm 3.9$  ka old topmost speleothem (Fig. 3). The paleomagnetic directions (D, I) are very close to the present magnetic field. Therefore we assume deposition of studied sediments within the Brunhes chron (<780 Ka) and the excursion may be correlated with excursions Jamaica-Pringle Falls (205–215 ka) and/or Calabrian Ridge 1 (315–325 ka; Langereis et al. 1997).

## 5. PALEONTOLOGY

The fragment of white ovate cuticle was found near sample HH230 in a crack in brown clays, close to cave wall. Part of fragment decomposed *in situ* to whitish powder. Sample was collected by L. Plan and P. Bosák on September 6, 2013. It was later send to A. Mock via Ľubomír Kováč (Košice, Slovakia).

The fragments of cuticle of ring-like shape clearly are parts of trunks (segments) of millipedes (Diplopoda). Organic parts of cuticle were lost or were substituted by anorganic material. Microstructure of prosomites and metasomites were also lost (like grooves, fine nodes, setae etc.). Sole bigger fragment of body shows noticeable nodes on metasomites. The shape of metasomite with node indicates it could be some representant of the millipede order Chordeumatida. In this locality, there is well-known occurrence of recent species from this order (Diplopoda: Chordeumatida: Attemsidae), *Polyphematia moniliformis* (Latzel, 1884), published by several authors, reviewed by Strouhal and Vornatscher (1975, pp. 472–475). Character of external morphology (size, shape) of this species (as same as other attemsiids) is similar to controlled fragments (other species recently dwelling this cave, *Haasea flavescens*, has somites without clear nodes). The probability that it is the same species is high.

Ecology of the attemsiid millipedes is specific: they are cave dwellers, but they occupy also surface and subsurface habitats closely connected with underground spaces with stable microclimate. Some genera and species are distributed mainly in Alps, especially in the east part (Austria, Slovenia). Most of them are endemites with small areas, surviving *in situ* probably for a long period (e. g., 2–3 species distributed in isolated area of the Western Carpathians and we supposed they are Tertiary relict, see Mock and Tajovský 2008) and using underground as refuges during periods with unfavorable climate. They are only partly adapted to underground (juvenile stages are almost without pigment) with possibility to live also on/at surface.

## 6. DISCUSSION OF RESULTS

Dating of cave sediments in the Hermannshöhle proved high cave dynamics in vadose regime with multiple filling and excavation phases as indicated by Th/U dates from speleothems ranging from ca 100 to over 600 ka. Paleomagnetic analysis of samples from Teichkluft profile showed N polarized magnetization and two very short R polarity intervals (excursions) in positions of samples HH219 to HH226 and HH41. As the interval of HH219–HH226 reveal higher coercivity fraction and its identity is still unknown (probable higher hematite/goethite contents), the R polarity is not proved. The R polarity interval of the HH41 sample represents a geomagnetic excursion without any doubt. The paleomagnetic directions (D, I) are very close to the present magnetic field. Therefore the deposition of studied sediments took place within the N-polarized Brunhes chron (<780 ka). Sediments are surely older than  $162.7 \pm 3.9$  ka old topmost speleothem. Than, the proved R-polarized excursion may be correlated with Jamaica-Pringle Falls (205–215 ka) or Calabrian Ridge 1 excursions (315–325 ka; Langereis et al. 1997).

Other Th/U date was obtained at the tourist trail opposite to Teichkluft entrance (ca 495 ka +67/-41 ka) in an altitude corresponding to the top of the Teichkluft profile. This might indicate that the Teichkluft was completely or nearly completely filled twice (before 163 and ca 495 ka) and once completely excavated (between ca 205/325 and ca 495 ka).

## 7. CONCLUSIONS

Detailed paleomagnetic analysis of sedimentary profile at Teichkluft showed that sediments are characterized by varying magnetic susceptibilities and NRM with increasing tendency of anisotropy parameter with increase of susceptibility. The component analysis identified 2 short R polarity intervals (0.41 m; 2.19–2.26 m) within samples with the N polarity. Rock magnetic and AMS measurements indicated mostly the presence of oblate, low coercivity magnetic fraction, presumably magnetite. However, the R polarity interval (2.19–2.26 m) revealed also other, higher coercivity fraction (maybe due to presence of hematite/goethite). The identity of this fraction is still unknown. The R polarity interval in 0.41 m represents a geomagnetic excursion without any doubt. The sedimentary profile with the R polarity interval in 0.41 m must be older than  $162.7 \pm 3.9$  ka old topmost speleothem. The paleomagnetic directions (D, I) are very close to the present magnetic field. Therefore we assume deposition of studied sediments within the Brunhes chron (<780 Ka) and the excursion may be correlated with Jamaica-Pringle Falls (205–215 ka) or Calabrian Ridge 1 excursions (315–325 ka; Langereis et al. 1997). Other Th/U date was obtained at the tourist trail opposite to Teichkluft entrance (ca 495 ka  $\pm$  67/-41 ka) in an altitude corresponding to the top of the Teichkluft profile. This might indicate that the Teichkluft was completely or nearly completely filled twice (before 163 and ca 495 ka) and once completely excavated (between ca 205/325 and ca 495 ka).

The fragments of cuticle of ring-like shape at the level of 2.30 m belongs to attensiid millipedes. The probability that fragments represent *Polyphematia moniliformis* (Latzel, 1884; Diplopoda: Chordeumatida: Attensiidae) known in the cave is high. It is supposed they are Tertiary relict (Mock and Tajovský 2008). It is not detected, if fragments represent relics of recent/subrecent animal entering open fractures in brown clays close to cave walls, or if they represent really fossil older than ca 163 ka.

### Acknowledgement

We are grateful to Hermannshöhle – Kirchberg am Wechsel for permission of field work and arrangement of lodging. We acknowledge the help of doc. RNDr. Ľubomír Kováč, PhD (University of Pavel Josef Šafařík, Košice, Slovakia) for finding of biology specialist for determination of organic remains.

The paleomagnetic analysis, evaluation and preparation of the report were carried out within the Plan of the Institutional Financing of the Institute of Geology ASCR, v. v. i. No. RVO67985831.

## 7. REFERENCES

- Bosák P., Pruner P., Kadlec J. (2003): Magnetostratigraphy of cave sediments: application and limits. – *Studia Geophysica et Geodaetica*, 47, 2: 301–330. Praha.
- Fisher R. (1953): Dispersion on a sphere. – *Proceedings of the Royal Society of London, Series A* 217: 295–305.
- Jelínek V. (1973): Precision A.C. bridge set for measuring magnetic susceptibility and its anisotropy. *Studia Geophysica et Geodaetica*, 17: 36–48.
- Jelínek V. (1981): Characterization of the magnetic fabric of rocks. – *Tectonophysics*, 79: T63–T67.
- Kirschvink J. L. (1980): The least-squares line and plane and the analysis of paleomagnetic data. – *Geophysical Journal of the Royal Astronomical Society*, 62: 699–718.
- Langereis C.G., Dekkers M.J., Lange G.J. de, Paterne M., Santvoort P.J.M. van (1997): Magnetostratigraphy and astronomical calibration of the last 1.1 Myr from an eastern Mediterranean piston core and dating of short events in the Brunhes. – *Geophysical Journal International*, 129: 75–94.

- Man O. (2008): On the identification of magnetostratigraphic polarity zones. – *Studia Geophysica et Geodaetica*, 52: 173–186.
- Mock A., Tajovský K. (2008): *Mecogonopodium carpathicum* n. sp. (Diplopoda: Chordeumatida: Attemsiidae), a new troglophilic millipede from Slovakia. – *Zootaxa*, 1778: 26-36
- Příhoda K., Krs M., Pešina B., Bláha J. (1989): MAVACS - a new system creating a nonmagnetic environment for palaeomagnetic studies. pp. 223-250. – In: Banda, E. (Ed.): *Paleomagnetismo – Palaeomagnetism Cuadernos de Geologia Iberica*. CSIC, Madrid, 1988-1989.
- Schober A., Plan L., Schulz D., Spötl Ch. (2013): Speleogenesis of a 3d-Maze cave (Hermannshöhle, Lower Austria). – in: Filippi M., Bosák P. (Eds.): *Proceedings of the 16<sup>th</sup> International Congress of Speleology, July 21–28, Brno*, Vol. 3: 408-411. Czech Speleological Society. Praha.
- Strouhal H., Vornatscher, J. (1975): Katalog der rezenten Höhlentiere Österreichs. – *Annalen des Naturhistorischen Museums in Wien*, 79: 401-542. ([http://www.landesmuseum.at/pdf\\_frei\\_remote/ANNA\\_79\\_0401-0542.pdf](http://www.landesmuseum.at/pdf_frei_remote/ANNA_79_0401-0542.pdf))
- Zupan Hajna N., Mihevc A., Pruner P., Bosák P. (2008): *Palaeomagnetism and Magnetostratigraphy of Karst Sediments in Slovenia*. – *Carsologica* 8: 1-266. Založba ZRC. Ljubljana.

**Paleomagnetic research of cave fill in Hermannshöhle, Austria.**  
Final Report

## **APPENDIX**

# **PHOTO PLATE**

### **List of photos**

**Photo 1** Lower segment – samples Nos. HH03 to HH110

**Photo 2** Segment HH03 to HH33

**Photo 3** Segment HH26 to HH58

**Photo 4** Segment HH54 to HH91

**Photo 5** Segment HH74 to HH110

**Photo 6** Lower middle segment – samples Nos. HH115 to HH125

**Photo 7** Lower middle segment – samples Nos. HH219 to HH244

**Photo 8** Upper middle segment – samples Nos. HH310 to HH389

**Photo 9** Lower upper segment – samples Nos. HH401 to HH420

**Photo 10** Topmost segment – samples Nos. HH470 to HH495

All photos by Pavel Bosák





**Photo 1** Lower segment – samples Nos. HH03 to HH110





**Photo 2** Segment HH03 to HH33



**Photo 3** Segment HH26 to HH58





**Photo 4** Segment HH54 to HH91



**Photo 5** Segment HH74 to HH110





**Photo 6** Lower middle segment – samples Nos. HH115 to HH125



**Photo 7** Lower middle segment – samples Nos. HH219 to HH244





**Photo 8** Upper middle segment – samples Nos. HH310 to HH389





**Photo 9** Lower upper segment – samples Nos. HH401 to HH420





**Photo 10** Topmost segment – samples Nos. HH470 to HH495